Journal of Physics: Conference Series **490** (2014) 012191 doi:10.1088/1742-6596/490/1/012191

Cumulation of a spherically converging shock wave in metals and its dependence on elastic-plastic properties, phase transitions, spall and shear fractures

E A Kozlov, A V Petrovtsev
Russian Federal Nuclear Center – Zababakhin Research Institute of Technical Physics, Snezhinsk, Chelyabinsk Region, Russia

E-mail: ea_kozlov@mail.ru

Abstract. Consideration is given to results of experimental and theoretical investigations how alpha-epsilon- phase transition in the unalloyed iron and the 30KhGSA steel and its absence in the austenitic 12Kh18N10T stainless steel influence processes under explosive deformation of spheres made of these materials. Polymorphous transition is shown to significantly effect on:
- amount of explosion-products energy transferred to a sphere,
- evolution of the converging-wave structure and its parameters, profiles of stress wave and temperature T(R,t) for some Lagrangian particles along the sphere radius,
- character of energy cumulation under spherical convergence of waves.

1. Introduction

The problem on the focusing of a spherically converging shock wave is a classical problem. G.Guderley [1] was the first to consider this problem for an ideal gas having equal initial density along the radius. Later, analogous self-similar solution was constructed by L.D. Landau and K.P. Stanyukovich [2,3]. Results of follow-on numerous investigations with a gas sphere having initial density that decreases or increases to its center were published in papers by G.M. Gandelman, D.A. Frank-Kamenetsky [4], F.L. Chernousko [5], K.V. Brushlinsky, Ya.M. Kazhdan [6], Yu.S. Vakhromeev [7], and Tyl I., Wlodarczyk [8].

All these investigations consider the case when properties of the matter closely correspond to the ideal gas. This is not just the situation we have in practice. Therefore, the follow-on works made attempts to estimate how the considered phenomenon and, more specifically, character of energy cumulation variation depend on real properties of the matter. E.I. Zababakhin contributed seriously to these investigations [9]. So, paper [10] considered the case with the heat-conducting gas and paper [11] – the case with the solid spheres. In the latter case a converging wave had the two-wave configuration due to shear strength or phase transition. Self-similar solutions constructed in [11] corresponded to the flow near the center when the principal plastic wave failed to catch up with the converging elastic or phase precursors. Idealized representations were used for the description of the elastic-plastic deformation and phase transition in the material at which the infinite cumulation is absent when these waves converge to the center. The idea on the finite energy cumulation, developed by E.I. Zababakhin, further was confirmed by experimental investigations [12,13] in which the spherical-shock-waves-recovery-experiments allowed rather detailed study how the cumulation character in the case of different-intensity stress waves convergence depends on real properties of materials.

Effects of energy cumulation decrease at the front of a converging stress wave in the above experiments due to the elastic-viscose-plastic deformation and alpha-epsilon-phase transition in the compressed-sphere material (iron) were computationally and theoretically studied in [14] and then – in [15, 16]. The purpose of this work is to obtain more detailed data on the aspect under consideration.

2. Materials, samples, and conditions of their explosive loading

Spheres made of iron, Steel 3, the quenched 30KhGSA steel (HRC=35...40), and the 12Kh18N10T steel [12,13,17-21] were investigated experimentally and theoretically. The diameters of these spheres were 40, 48, 60, 64, 166, and 184 mm. Detonation of the RDX- or HMX-based explosive layers with the outer radius R_{HE} = 40 or 110 mm and different initial thicknesses was used for explosive loading of these spheres. Note that as for the shock-wave properties (figure 1) – both possible formation of multi-wave configurations and energy dissipation amount under shock-wave deformation, the investigated materials can be arranged as follows: (i) the 12Kh18N10T steel having no polymorphous alpha-epsilon-phase transition and having small values of the dynamic yield stress (Y_A≈0.25 GPa...1.0 GPa where the first value corresponds to the stress at the elastic precursor with the 0.45 GPa amplitude and the second value takes into account strain hardening in stress waves without influence of pressure and temperature); (ii) Iron and Steel 3 having polymorphous transitions and approximately the same (Y_A≈0.65 GPa) shear stresses [22-24]; (iii) the 30KhGSA steel quenched up to HRC=35...40 having the same alpha-prime-epsilon-phase transition at essentially higher (Y_0≈1.0...2.3 GPa, σ^{HEL}=1.8 GPa) shear stresses [25,26].

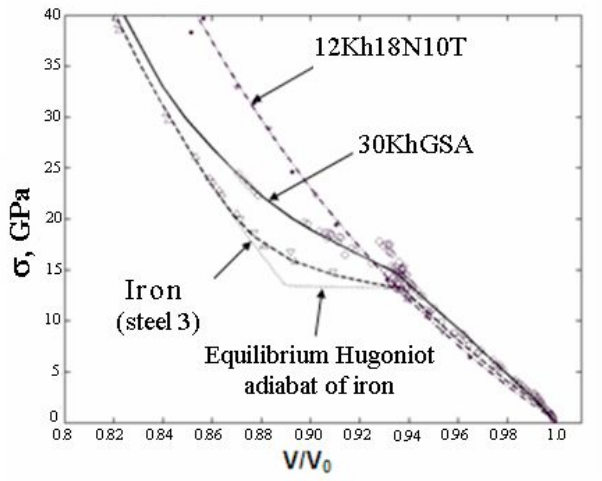

Figure 1 – Hugoniot adiabat for iron [22-24] or steel 3 [12], the quenched 30KhGSA steel [25, 26] and the same steel as received [12], as well as for the 12Kh18N10T steel [12,27].

Furthermore, metastability of the alpha-prime-epsilon- (α'-ε) phase transition is noted to have a more pronounced character in the quenched 30KhGSA steel [25, 26] as compared to that of iron [22-24] and this results in a more pronounced dissipation of energy in the loading – unloading cycle.

3. Numerical computations

Behavior and properties of iron and steels were described with the help of models based both on the multi-phase equations of state and the governing relationships used to describe the high-rate elastic-viscous-plastic deformation, kinetics of phase transitions, incipience and development of fractures and their recompaction, as well as to describe interrelation between these processes.

If the multi-phase equations of state [28,29] describe thermodynamic properties of the solid (three - α, γ, ε - for iron and one – for the 12Kh18N10T steel) and liquid phases, then the equations of state for liquid phases – are wide-range equations that take into account evaporation as well. The model well described in [16,30] was used to simulate the elastic-viscous-plastic properties, phase transitions, and fractures. This model takes into account strain hardening of a material similarly to [31], power-law dependence of shear stresses on strain rate [32], the Bauschinger effect [31,33], and influence of fractures and phase transitions available in the material on the elastic-viscous-plastic properties of this

material. Phase transitions are described based on the relaxational-type kinetic equations [34] which are generalized to the case of several transitions simultaneously proceeding in a material particle. Characteristics of the model are such that the model takes into account real metastability and dependence of time required for transition to proceed in the test materials [12,16,24,25,30] on the degree of non-equilibrium states. A fracture is described by kinetic equations of nucleation and growth (similar to those in [35]), which are also capable to describe the reverse process, i.e. recompaction of these fractures. The model takes into account hardening of materials due to polymorphous transitions in them under shock-wave loading [36] and their softening under melting. Parameters of models were determined based on measurement results for shock compressibility, sound velocities, and stress wave profiles in the materials under consideration.

Such a computational setup was used, which took into account details of the experimental systems design and the loading process was simulated up to rather long time moments that correspond to their actual stop.

Computations were performed with the help of the VOLNA program complex which is intended for 1D-numerical simulation of continuum dynamics [37] and includes the above models. Potentialities of this program complex in determining the exact shock fronts and characteristics of rarefaction waves in calculations of the flow inside the spheres were not previously applied as the models that take into account strain rate of a material and kinetics of processes were usually used. The required accuracy in computations of shock-wave amplitudes especially near the center where they reach high values, as well as sufficiency of energy dissipation at the front of a converging wave (for correct description of temperature and phase state of particles in a material) was ensured through the use of a rather fine grid (≈5000 spacings with the abovementioned sizes of samples).

4. Results and their discussion

4.1 Simulation of experiments with the explosive system having R_{HE}= 110 mm

General data on the character of processes in the samples are shown in figures 2, 3 for the iron sphere with the 166-mm initial diameter.

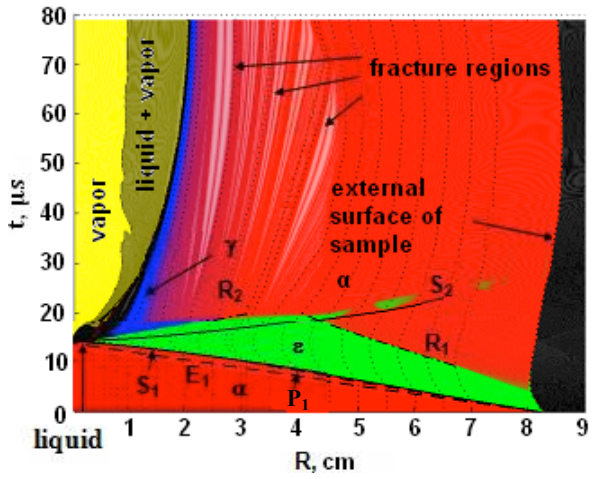

Figure 2 – R-t diagram of the waves and contact boundaries movement in the experiment with the iron sphere having 166-mm initial diameter

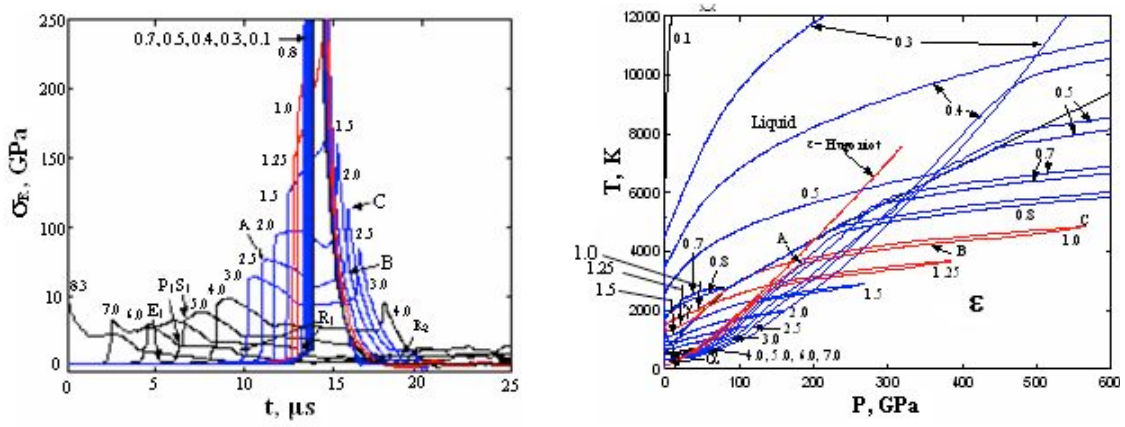

a) b)

Figure 3 – Time profiles of stresses (a) and P-T histories of particles strain (b) in the iron sample with the 166-mm diameter.
Numbers near the curves – Lagrangian radii of particles in cm.

A pressure pulse induced by detonation of the HE layer at the external surface of the sphere creates a stress wave propagating towards the center. At the initial state, the wave amplitude decreases with the wave propagation due to unloading from the side of the scattering explosion products (figure 3a).

Depending on the loading intensity and impulse duration, conditions are created for the generation in iron of the multi-wave configuration with the formation, along with the principal plastic wave S_1, of the elastic E_1 (at $\sigma_R \leq 70$GPa in iron or at $\sigma_R \leq 40$GPa in 12Kh18N10T steel) and phase P_1 (at $\sigma_R \leq 35$GPa in iron, no in steel 12Kh18N10T) precursors. The structure of the waves being formed and those converging to the center, as well as the level of their spatial divergence depend on the explosive loading conditions. In the principal plastic wave, iron particles transit from the state of the initial alpha-phase into the epsilon-high-pressure phase. In further propagation of the waves, the amplitude and velocity of the principal wave S_1 begin to grow because of spherical convergence. So, at a certain radius, the multi-wave configuration can totally or partially stop to exist as the front of the principal shock wave catches up with the phase precursor and then with the elastic precursor. When the principal wave amplitude becomes $\sigma_R \geq 200$ GPa, the calculation shows that the matter gets melted at the principal wave front. When the wave is reflected from the center, behind the diverging-wave front one observes material unloading into the formed cavity with obtaining the vapor and then, with the distance from the center, the vapor-liquid mixture and the high-temperature gamma phase (figure 2). The reverse transition of the epsilon– to– alpha-phase takes place in the sample's peripheral part constituting the major part of the sample. The rarefaction waves propagating from the cavity and from the external surface of the sample incorporate rarefaction shock waves designated in figure 2 as R_2 and R_1, respectively. Interaction of rarefaction waves lead to the formation in the sample of the fracture regions concentrically located above the cavity. Then due to the cast-iron case that is located above the HE layer and generates a number of additional compression pulses at the surface of the sample, the early formed spall fractures can be recompacted (figure 2). This character of high-rate deformation, fracture, and recompaction of materials after spherical explosive loading was noted in [12,13,19,20] during metallographic and electron-microscopic studies of recovered samples of Fe and steels.

P-T histories of particles strain in the P-T diagram (figure 3b) show that the main portion of the melt in the iron sample with ∅ 166 mm is formed under unloading of the matter heated by the principal wave rather than melting at the shock wave front. Though pursuant to calculations for iron, the shock wave amplitude $P^H \approx 180$GPa corresponds to the melting onset under unloading and the wave amplitude $P^H \approx 200$GPa corresponds to the melting at the shock wave front.

Figure 3a gives time histories for the radial component of stresses for certain Lagrangian particles. One can see that loading of material particles has a rather complicated multi-wave character. Thereby near the center, compression waves formed by the flow converging to the center are observed at the compression profiles between shock fronts of the converging multi-wave configuration, as well as between the front of the principal wave and that of the wave reflected from the center. Due to multi-wave and substantially non-shock character of deformation of material particles they demonstrate seriously less entropy and thus maximum temperatures in these particles are substantially lower under the same pressures if compared with temperatures at Hugoniot adiabats that correspond to their shock compression by a single wave. Quasi-isentropic nature of particles compression and variations of this nature due to cumulation under the wave convergence depend on the materials properties and the loading profile.

The pulse amplitude and duration can seriously change the character of multi-wave configurations realized in the iron sphere, as well as the spacing between waves in this sphere. For example, numerical simulation demonstrates that with the increase of the HE layer thickness due to the decrease in the diameter of the loaded iron sphere from 184 down to 166 mm in an appropriate explosive system [13,20,21], mass of the molten central area in this sphere increases 15 times. This is associated with the fact that with the 184-mm diameter of the sphere, the elastic and phase precursors run far ahead the converging principal wave and the single-wave mode of particles loading fails to form while in the second case (figure 2) the area of phase precursor existence is rather small.

4.2 Simulation of experiments with explosive systems having R_{HE}= 40 mm

Figures 4 and 5 give the results of numerical simulation for experiments [13,17] with explosive loading of the 64-mm diameter spheres made of different materials.

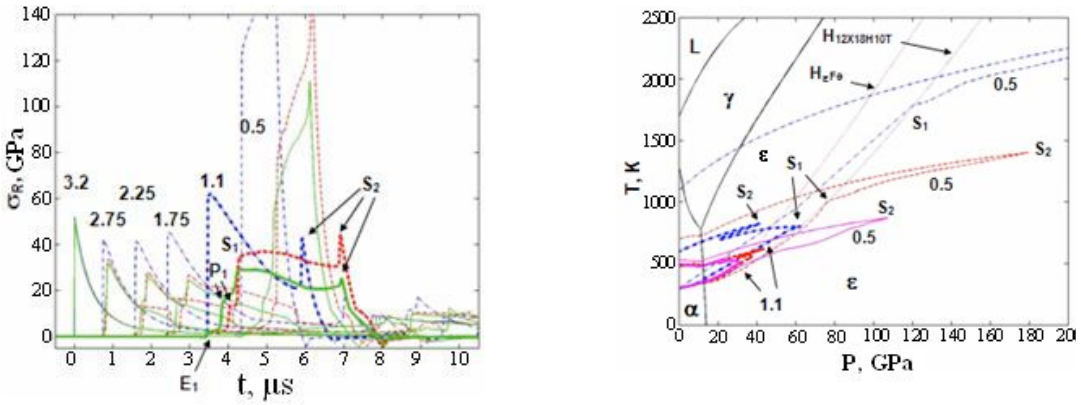

a) b)

Figure 4 – Time profiles of stresses (a) and trajectories how particles of steel grades under consideration deform in the pressure-temperature coordinates (b) for explosive experiments [13,17] with the 64-mm diameter spheres. Calculated data for the quenched 30KhGSA steel are shown as solid lines, for iron – as dashed lines, and for the 12Kh18N10T steel – as dash-dotted lines. Numbers near the curves – are Lagrangian radii of particles in centimeters. Thick solid lines in the P-T diagram (b) show stability areas for the solid and liquid phases of iron. The melting line for the 12Kh18N10T steel in this pressure area is close to the melting line of iron.

Figure 4a shows that in these experiments with samples of Steel 3 and the quenched 30KhGSA steel, the converging wave represents a three-wave configuration at medium radii and only one front is observed in the 12Kh18N10T steel. Meanwhile, the temperature decrease for the material compressed by the converging wave is most evident in the first two cases.

At the initial stage of motion, the converging wave attenuation is quite evident and it becomes even more evident in steels with polymorphous transitions especially in the quenched 30KhGSA steel. And the cumulation effect for these materials at the next stage of motion develops much later. So, the initial amplitude of the wave "recovers" due to the spherical convergence only at a rather deep radius R≈6 mm (or $0.15R_{HE}$) if compared with the similar radius R≈15 mm (or $0.375R_{HE}$) for the 12Kh18N10T steel. The noted differences in characteristics of the converging wave attenuation are also observed in the diverging wave traveling. In the case with the quenched 30KhGSA steel, the amplitude of this wave near the external surface of the sample becomes very small. This indicates that the reverse transfer of energy to the explosion products under sphere unloading in this case turns out to be much weaker. Table 1 gives quantitative data on the above effects.

Table 1 – Calculated characteristics of the converging and reflected waves in the samples

Material	Trajectory, mm	Converging wave		Diverging wave	
		σ_{S1}, GPa	T_{S1}, K	σ_{S2}, GPa	T_{S2}, K
12Kh18N10T	2.25	41.5	568 (553[1])	10.2(6.5[2])	
	1.1	62.1	800(798)	43.1(21.9)	
	0.5	122	1787(1778)	257(104)	2406
Iron	2.25	28.1	501	6.4(3.0)	
	1.1	34.1	528	44.6(14.1)	
	0.5	77	996(1363)	182(49)	1404
30KhGSA HRC 35…40	2.25	25.9	475	4.1(1.9)	
	1.1	29.0	471	25.5(3.7)	
	0.5	54.7	610(895)	111(11)	874

[1] Temperature at the hydro dynamical Hugoniot adiabat
[2] Jump of a radial stress component in the reflected wave

All noted factors, i.e. decrease of the wave amplitude due to stronger attenuation, weaker cumulation, and more isentropic character of loading, lead to the decreased values of loading amplitudes and decreased values of temperatures for iron particles and particles of the 30KhGSA steel in the central area. Hence, the amount of the molten matter for these materials after the cavity formation seriously decreases if compared to the 12Kh18N10T steel (Table 2) with rather close melting temperatures at P=0 in the equations of state for these materials and namely: T_{m0}=1672 K for the 12Kh18N10T steel and T_{m0}=1696 K for iron. Actually, in the case with the quenched 30KhGSA steel, in the explosive loading mode with the 64-mm sphere, the molten area is very small (in practice it is absent at all) and the cavity is formed owing to the fracture of the material in the solid phase under uniform extension just as for example in [38].

Table 2 – Data on energy transferred to the sphere and on sphere deformation after explosion

Material	Final radius, mm		Calculated radius of melting zone, mm	Transferred energy, kJ	
	Experiment [13]	Computation		Experiment [35]	Computation
12Kh18N10T	32.46 (1.0144[1])	32.67 (1.021[1])	0.33 (0.25[2])	102 (1.000[3])	136 (1.000[3])
Iron (Steel 3)	32.34 (1.0064)	32.44 (1.014)	0.16 (0.13)	115 (1.137)	155 (1.138)
30KhGSA HRC 35…40	32.26 (1.0081)	32.22 (1.0069)	0.052 (0.042)	129 (1.269)	176 (1.290)
Copper	32.91 (1.0285)	32.97 (1.030)		100 (0.984)	134 (0.980)

[1] Deformation of the outer radius of the sphere in per cents
[2] Boundary of the complete-melting area
[3] Relative value if compared with the sphere of the 12Kh18N10T steel

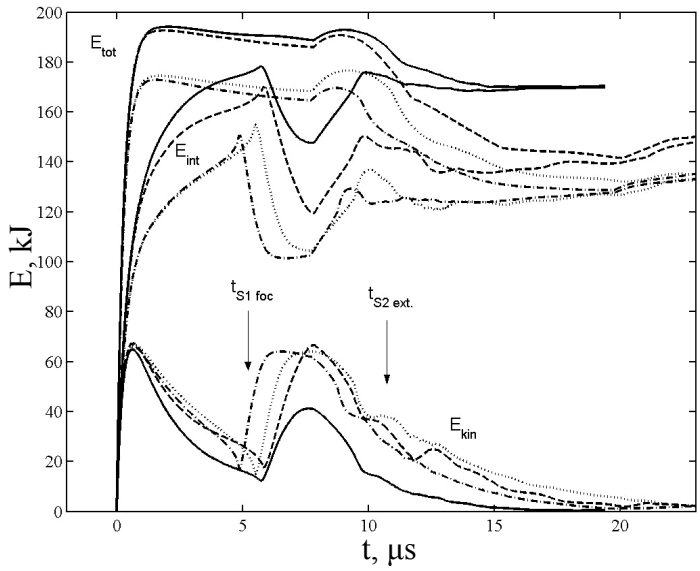

Figure 5 – Time variations of kinetic, internal, and total energy of spheres from the quenched 30KhGSA steel (solid lines), iron or Steel 3 (dashed lines), the 12Kh18N10T steel (dash-and dotted lines), and copper (dotted line).

Figure 5 shows a time-dependent integral quantity of the kinetic and internal energy of spheres from different materials, as well as a time-dependent total energy that corresponds to the work of explosion products at the surface of these spheres. Calculation data are additionally given for copper, i.e. material with no polymorphous transitions and with the minimal ($Y_A \approx 0.12...0.3$ GPa) shear strength from among all materials under consideration. As seen, at the initial stage of loading due to greater compressibility, non-equilibrium nature of the polymorphous alpha-epsilon-phase transition, and rather high shear stresses, the spheres from iron and the 30KhGSA steel get seriously greater part of explosion products energy as compared with the spheres from materials having no phase transition. In progress of the sphere deformation, the stronger energy dissipation takes place in the quenched 30KhGSA steel due to greater non-equilibrium of the α'-ε phase transition and high shear stresses;

thus, the reverse energy transfer to explosion products decreases. The internal energy in the 30KhGSA sphere gets larger and the kinetic energy – grows smaller as compared with the iron sphere and also spheres from other materials. This difference is observed to be maximum after the reflected wave arrives at the external surface of the sphere. Due to less cumulation of the converging wave, the internal-to-kinetic energy transfer when the wave is reflected from the center of the sphere from this material is noted to be minimal. Table 2 gives qualitative data on the energy E transferred by explosion products to the spheres. As seen, the calculated relation E for different materials is very close to the calorimetric measurement results presented in [17]. In addition, a qualitatively correct relation is observed between the final dimensions of spheres and, respectively, the dimensions of cavities just as in experiments [13,20]. Certain differences in absolute values can be associated with the use of 1D approach in computations and with possible 3D losses in experiments [21]. Further advancement of the computational and theoretical description, as well as experimental techniques to diagnose different stages of phenomena under study seems reasonable.

5.Conclusion

Experiments and their numerical simulations confirmed strong dependence of the energy cumulation character at the front of the converging shock wave on the polymorphous transition in iron and steels.

6. References

[1] Guderley G 1942 Starke kugelige und zylindrische Verdichtungsstöße in der Nähe des Kugelmittel punkte bzw. der Zylinderachse *Luftfahrtforschungsanstalt* **19,** 9, 302
[2] Landau L D and Stanyukovich K P 1945 See Stanyukovich K P 1955 Nonsteady flow of continuum. *(M.: Gostekhteorizdat, in Russian)*
[3] Landau L D and Lifshits E M 1986 *Hydrodynamics. Theoretical Physics* M.: Nauka, vol 6.
[4] Gandelman G M and Frank-Kamenetsky D A 1956 *Rus. J. Doklady Akademii Nauk (Reports Russian Academy of Science)* **107** issue 6 811
[5] Chernousko F L 1960 Converging shock waves in a variable-density gas *Rus. J. Applied Mathematics and Mechanics* **24** issue 5, 885
[6] Brushlinsky K V and Kazhdan Ya M 1963 On self-similar solutions of some gas-dynamic problems *Rus. J. Advances of Mathematical Sciences* **18** issue 2 3
[7] Vakhromeev Yu S 1966 Cumulation of shock waves in non-uniform medium *Rus. J.Applied Mathematics and Mechanics* **30** issue 4 774
[8] Tyl I and Wlodarczyk 1985 An analysis of the concentric shock wave in a nonhomogeneous polytrophic gas *J. Technical Physics* **26** issue 1.
[9] Zababakhin E I 1965 Cumulation of energy and its boundaries *Rus. J. Advances of Physical Sciences* **85** issue 4 721
[10] Zababakhin E I and Simonenko V A 1965 Converging wave in a heat-conducting gas *Rus. J. Applied Mathematics and Mechanics* **29** issue 2 334
[11] Zababakhin E I and Zababakhin I E 1988 Infinite cumulation phenomenon (*M.: Nauka)*
[12] Kozlov E A 1992 Shock adiabat features, phase transition macrokinetics, and spall fracture of iron in different phase states *High Pressure Research* **10** 541
[13] Kozlov E A 1992 Experimental verification of E.I.Zababakhin hypothesis concerning limitation of energy cumulation in the spherically converging shock-wave front in medium with phase transitions *Shock Compression of Condensed Matter – 1991*, eds S C Schmidt et.al (Elsevier Science Publishers B.V.) pp 169-172
[14] Kozlov E A and Zhukov A V 1994 Phase transitions in spherical stress waves *High Pressure Science and Technology – 1993,* eds S C Schmidt, J W Shaner, G A Samara and M Ross (NewYork: American Institute of Physics) pp 977-980.
[15] Afanasieva S A, Belov N N and Konyaev A A 1998 Computer simulation of materials behavior under shock-wave loading (*Rus.* J. *Izvestia Akademii Nauk), Proceedings Academy of Science. Solid-State Mechanics* **5** 115
[16] Kovalenko G V and Petrovtsev A V 2001 Numerical simulation of elastic-viscous-plastic properties, phase transitions, and fractures in iron *VI Zababakhin Scientific Talks* (Snezhinsk,

Chelyabinsk region, Russia, September 24-28 2001) pp 208-209 (Abstract, full text: <www.vniitf.ru/rig/konfer/6zst/reports/s5/5-45.pdf>).

[17] Vildanov V G, Gorshkov M M, Kozlov E A, Tkachev O V and Yusupov D T 2003 Solid-state calorimeter technique to measure residual energy of spheres and shells after explosive compression *VII Zababakhin Scientific Talks* (Snezhinsk, Chelyabinsk region, Russia, September 8-12, 2003) pp 185 (Abstract, full text: <www.vniitf.ru/rig/konfer/7zst/reports/s5/5-35.pdf>)

[18] Kozlov E A , Taluts N I, Dobromyslov A V 2005 High-rate deformation of armco-iron loaded by spherically converging shock waves *Physics of substance extreme state* (Chernogolovka, Moscow region: Published by Rus. Institute of Chemical Physics Problems) pp 75-77

[19] Dobromyslov A V, Kozlov E A, Litvinov B V and Taluts N I 2007 High-rate deformation of armco iron under loading by spherically converging shock waves *Proceedings of Russian Academy of science Doklady Physics* (Engl. transl.) **52**, issue 8 418

[20] Kozlov E A, Dobromyslov A V, Taluts N I and Voltz K 2012 Effect of spherically converging shock waves on deformation and phase behavior of high-purity iron *J. Physics of Metals and Metallography* (Engl. transl.) **113** issue 10 1007

[21] Kozlov E A, Brichikov S A, Boyarnikov D S, Kuchko D P and Degtyarev A A 2011 Special features in convergence dynamics of steel shells under their explosive loading. results of laser-interferometric measurements *J. Physics of Metals and Metallograph* (Engl. transl.) **112** issue 4 389

[22] Bancroft D, Peterson E L, Minshall S 1956 Polymorphism of iron at high pressure *J. Appl. Phys* **27** 291

[23] Barker L M, Hollenbach R E 1974 Shock wave study of the α-ε phase transition in iron *J. Appl. Phys* **45** 4872

[24] Kozlov E A, Telichko I V, Gorbachev D M, Pankratov D G, Dobromyslov A V and Taluts N I 2005 On the metastability and incompleteness of the α–ε phase transformation in unalloyed iron under the threshold loading pulses: specific features of the deformation behavior and structure of armco iron *J. Physics of Metals and Metallography* (Engl. transl.) **99**, issue 3 *300*

[25] Kozlov E A, Tarzhanov V I, Telichko I V and Pankratov D G 2012 Shear and spall strength of hardened 30KhGSA steel under explosive loading in the range of solid-solid phase transformation *Rus. J. Deformation and Fracture of Materials* **8** 32

[26] Kozlov E A 2012 2D-, and 3D-explosive experiments for verification of spall and shear strengths models for some steels *17th APS Conference on Shock Compression of Condensed Matter (* Chicago, Illinois, USA, June 26 – July 1, 2011) eds M L Elert, W T Buttler, J P Borg, J L Jordan and T J Vogler (Melville, New York: AIP CP 1426) pp. 945-948

[27] Belyakova M Yu, Zhernokletov M V, Sutulov Yu N and Trunin R F 1991 Shock compression of metal alloys (*Rus. J. Izvestia Akademii Nauk) Physics of the Earth* **1** 99

[28] Dremov V V, Kutepov A L, Petrovtsev A V, and Sapozhnikov A T 2002 Equation of state and phase diagram of iron *Shock Compression of Condensed Matter – 2001(Atlanta, Georgia, USA, 24-29 June 2001)* eds M D Furnish, N N Thadhani and Y Horie (Melvill, NewYork: AIP Conference Proceedings #620) pp 87-90

[29] Zadorozhny G A, Petrovtsev A V and Dremov V V 2005 Equation of state for the 12Kh18N10T steel *VII Khariton Scientific Talks (Sarov, Nizhniy Novgorod region, Russia, March 14–18, 2005*)

[30] Zadorozhny G A, Kovalenko G V and Petrovtsev A V 2003 Modeling of the polymorphous α-ε phase transition in iron in a wide range of states. *VII Zababakhin Scientific Talks (Snezhinsk, Chelyabinsk region, Russia, September 8-12, 2003)* p 183 (Abstract, full text - <www.vniitf.ru/rig/konfer/7zst/reports/s5/5-45.pdf>)

[31] Steinberg D J, Cohran S G and Guinan M W 1980 A constitutive model for metals at high-strain rate *J. Appl. Phys* **51** 1498

[32] Swegle J W and Grady D E 1985 Shock viscosity and the prediction of shock wave rise times *J. Appl. Phys* **58** 692

[33] Moss W C and Glenn L A 1984 A Bauschinger effect model for use in large computer codes *Shock Waves in Condensed Matter – 1983* eds J R Asay, R A Graham, and G K Straub (American Institute of Physics) pp 133-136

[34] Andrews D J 1971 Calculation of mixed phases in continuum mechanics *J. Comp. Phys* **7** 310

[35] Belov N N, Korneev A I and Nikolaev A P 1985 Numerical analysis of fracture in pulsed-loaded plates. *Rus. J. Applied Mechanics and Technical Physics* **3** 132

[36] Bychenkov V A, Kovalenko G V, Kozlov E A, Lobachev S V, Petrovtsev A V and Zhugin Yu N 2003 Spallation of armco-iron and 30KhGSA steel under explosive loading in the region of α-ε phase transition: experiment and calculation *Proceeding of Fifth International Symposium on Behaviour of Dense Media under High Dynamic Pressures (Saint-Malo, France, 23-27 June, 2003 vol 1*) pp 431-434

[37] Kuropatenko V F, Kovalenko G V and Kuznetsova V I 1989 Complex of VOLNA codes and non-uniform finite difference method to calculate the compressible media flow *Russian J. Issues of Atomic Science and Engineering. Series: Techniques and Codes for Numerical Solution of Mathematical Physics Problem,* issue **2** 9

[38] Bakhrakh S M, Kovalev N P, Nadytko B A, Novikov S A and Chernyshev A K 1974 Study of plastic and strength properties of copper in conditions of uniform extension *Rus. J. Doklady Akademii Nauk* **215**, issue 5 1090